

Myosin–actin interaction plays an important role in human immunodeficiency virus type 1 release from host cells

(viral budding/myosin light chain kinase/wortmannin/cytochalasin D)

HIROYUKI SASAKI*, MARIKO NAKAMURA†, TSUNEYA OHNO†, YUZURU MATSUDA‡, YASUKATSU YUDA§, AND YOSHIKI NONOMURA¶||

*Division of Morphology, Institute of Medical Science and †Department of Microbiology, The Jikei University School of Medicine, Minato-ku, Tokyo 105, Japan; ‡The Tokyo Research Laboratories, Kyowa Hakko Co., Ltd., Machida-shi 194, Japan; §Institute of Drug Development, Meijiseika K.K., Yokohama 222, Japan; and ¶First Department of Pharmacology, Faculty of Medicine, University of Tokyo, Tokyo 113, Japan

Communicated by David D. Sabatini, New York University Medical Center, New York, NY, October 24, 1994

ABSTRACT We examined the potential role of myosin and actin in the release of human immunodeficiency virus type 1 (HIV-1) from infected cells. Wortmannin (100 nM to 5 μ M), an effective inhibitor of myosin light chain kinase, blocked the release of HIV-1 from infected T-lymphoblastoid and monocytoïd cells in a concentration-dependent manner. Cytochalasin D, a reagent that disrupts the equilibrium between monomeric and polymeric actin, also partially inhibited the release of HIV-1 from the infected cells. At the budding stage, myosin and HIV-1 protein were detected in the same areas on the plasma membrane by using dual-label immunofluorescence microscopy and immunoelectron microscopy. In the presence of 5 μ M wortmannin, viral components were observed on the plasma membrane by using immunofluorescence microscopy and electron microscopy, implying that wortmannin did not disturb the transport of viral proteins to the plasma membrane but rather inhibited budding.

The infection and release of human immunodeficiency virus (HIV) from lymphocytes, monocytes, and macrophages involves several distinct steps including binding to a specific surface receptor, entry into the host cell, reverse transcription of the RNA genome, replication, transcription, protein synthesis, intracellular transportation, recognition of release sites, and budding (for reviews, see refs. 1–3). Although research during recent years has yielded many important insights into several of these stages in the life cycle of HIV, very little is known about the final step, where infected viruses are released from cells.

Recently our laboratory has obtained evidence that cytoskeletal proteins, including myosin II (hereafter referred to as myosin) play a role in a variety of cellular exocytic events (4–6), especially in transmitter release from neuronal cells (7, 8). These studies employed two tools: wortmannin, a potent inhibitor of myosin light chain kinase (MLCK) (9), and an anti-myosin antibody that specifically recognizes the heavy chain of smooth muscle and nonmuscle myosin (ref. 6 and Y.N., unpublished work). Actin is a ubiquitous cytoskeletal protein of eukaryotic cells and has various functional roles in the cell (10). In paramyxovirus-infected cells, actin has been suggested to play a role in the transport of synthetic viral RNA and proteins to the surface membrane of the host cell (11–13), but the participation of myosin in the viral synthetic processes from inoculation to virion release has not yet been elucidated. Cytochalasin D is a useful tool for testing of the participation of actin in various cell functions, because it disturbs the equilibrium between monomeric and polymeric actin by capping the barbed end of actin filament and lowering the amount

of ATP-bound monomer actin (10, 14–18). In fact, recently, a critical role for actin filaments was suggested in endocytosis from the apical surface of polarized epithelial cells by using cytochalasin D (19). Since viral budding can be considered an exocytic event, we decided to use wortmannin and cytochalasin D to examine the mechanism of HIV budding.

MATERIALS AND METHODS

Materials. Uninfected T-lymphoblastoid H9 cells and monocytoïd U937 cells infected with HIV-1 IIIB were maintained in RPMI 1640 medium containing 10% (vol/vol) heat-inactivated fetal bovine serum and 2 mM L-glutamine. HIV-1 IIIB was obtained from the AIDS Research and Reference Reagent Program, National Institutes of Health, Bethesda. Wortmannin was prepared as described (9). Wortmannin, KT5926 (Kyowa Hakko Kogyo, Tokyo) (20, 21), and cytochalasin D (Sigma) were dissolved in dimethyl sulfoxide to prepare stock solution.

Antiviral Assay. H9 cells primarily infected with HIV-1 IIIB on day 4 and chronically HIV-1 IIIB-infected U937 cells were suspended at 2.5×10^5 cells per ml. Serially diluted wortmannin (2 μ l), KT5926 (2 μ l), or cytochalasin D (2 μ l) was then added to 198 μ l of the cell suspension, and the suspensions were incubated for various times. The supernatant fraction (1500 rpm for 5 min) of the culture medium and sedimented cells were harvested for the reverse transcriptase (RT) assay and the 3-(4,5-dimethylthiazol-2-yl)-2, 5-diphenyltetrazolium bromide (MTT) assay, respectively.

The RT assay was performed as described (22). The supernatant fraction (10 μ l) containing HIV-1 particles was disrupted with 10 μ l of detergent solution (50 mM Tris-HCl, pH 8.0/10 mM dithiothreitol/300 mM KCl/0.5% Triton X-100). After a 15-min incubation at 4°C, 25 μ l of RT buffer [50 mM Tris-HCl, pH 8.0/10 mM MgCl₂/5 mM dithiothreitol/poly(rA)·(dT)_{12–18} (Pharmacia; 0.25 unit/ml)/[³H]dTTP (American Radiolabeled Chemicals, St. Louis; 15 μ Ci/ml; 1 Ci = 37GBq)] was added. The reaction mixtures were incubated at 37°C for 18 h and the incorporation of [³H]dTMP was measured in a scintillation counter (Beckman).

The MTT assay was performed as described (23).

Gel Electrophoresis and Immunoblot Analysis. Approximately 1×10^6 cells were disrupted by addition of 50 μ l of SDS sample buffer and boiled for 5 min. SDS/PAGE was carried out with 6% gels for detection of myosin and 14% gels for actin; the samples were then blotted onto nitrocellulose membranes (0.25- μ m pore size, Schleicher & Schuell), incubated

with blocking solution [10% (vol/vol) skim milk/2.5% (wt/vol) bovine serum albumin in phosphate-buffered saline (PBS)] for 30 min, and reacted with a rabbit anti-myosin polyclonal antibody produced in our laboratory (6) or a mouse anti-actin monoclonal antibody (Boehringer Mannheim) in the blocking solution for 3 h at 37°C. Membranes were subsequently washed with 0.1% Nonidet P-40 in PBS, reacted with a horseradish peroxidase (HRP)-conjugated goat anti-rabbit IgG or -mouse IgG (Organon Teknika-Cappel) in the blocking solution for 1 h at 37°C, washed, and reacted with 4-chlor-1-naphthyl phosphate. Anti-myosin antibody reacted intensively and specifically with mammalian nonmuscle myosin heavy chain.

Immunofluorescence Microscopy. H9 cells primarily infected with HIV-1 IIIB on day 4 were incubated with 5 μ M wortmannin for 24 h. The cells were sequentially fixed with 1% paraformaldehyde/0.1 M sodium phosphate (pH 7.2) and with acetone, each for 5 min at 4°C. The cells thus fixed were washed in PBS, placed on poly(L-lysine)-coated glass slides, and treated with 0.5% Triton X-100 in PBS for 5 min at 4°C. After incubation for 30 min at room temperature with blocking solution containing 10% (vol/vol) normal goat serum and 2.5% bovine serum albumin in PBS, cells were incubated for 1 h at room temperature in blocking solution containing mouse anti-HIV-1 gp120 monoclonal antibody (24) or mouse anti-HIV-1 p24 monoclonal antibody produced in our laboratory. After extensive washing in PBS, the cells were labeled for 1 h at room temperature with fluorescein isothiocyanate (FITC)-conjugated goat anti-mouse IgG (diluted 1:100) (Organon Teknika-Cappel) in the blocking solution.

For dual-label immunofluorescence microscopy, HIV-1 IIIB-infected H9 cells were incubated for 3 h at 37°C with rabbit anti-myosin polyclonal antibody (6) or mouse anti-actin monoclonal antibody (Boehringer Mannheim) in the blocking solution and then incubated for 1 h at room temperature with the IgG fraction of HIV-1-infected patient serum purified in our laboratory. After extensive washing in PBS, the cells were labeled for 1 h at room temperature with FITC-conjugated goat anti-rabbit IgG or -mouse IgG and rhodamine-conjugated goat anti-human IgG (diluted 1:100) (Organon Teknika-Cappel) in the blocking solution. Cells were examined with a Nikon Microphoto-FXA fluorescent microscope.

Electron Microscopy. For conventional electron microscopy, H9 cells primarily infected with HIV-1 IIIB on day 4 were incubated with 5 μ M wortmannin for 24 h. The cells were doubly fixed with 1.2% glutaraldehyde/0.1 M sodium phosphate (pH 7.2) and in 1% osmium tetroxide/0.1 M sodium phosphate (pH 7.2) and dehydrated with a graded series of ethanol. Cells were then embedded in epoxy resin. Ultrathin sections were stained with uranyl acetate and lead citrate and observed with a Hitachi H-7000 transmission electron microscope.

For immunoelectron microscopy, HIV-1 IIIB-infected H9 and U937 cells were fixed and pretreated as described for immunofluorescence microscopy. After incubation with the blocking solution, cells were incubated for 3 h at 37°C with rabbit anti-myosin polyclonal antibody in the blocking solution. After extensive washing in PBS, the cells were labeled for 1 h at room temperature with HRP-conjugated goat anti-rabbit IgG (Organon Teknika-Cappel) in the blocking solution and reacted with 3, 3'-diaminobenzidine and H₂O₂. Cells were postfixed with osmium tetroxide in 0.1 M sodium phosphate (pH 7.4), dehydrated with ethanol, and embedded in Epoxy resin. Unstained thin sections were observed with the transmission electron microscope.

RESULTS AND DISCUSSION

We first investigated the effects of wortmannin on HIV-1 release in cultures of primary infected H9 cells. H9 cells were

treated with wortmannin 96 h after inoculation of the cells with the HIV-1 IIIB, and supernatant fraction of the culture medium containing HIV-1 was harvested at various times thereafter. We quantified viral release by measuring RT levels in the supernatant fractions. Progeny viruses started to be released from H9 cells \approx 100 h after infection. Wortmannin treatment resulted in the concentration-dependent inhibition of HIV-1 release, as reflected in the RT activities in samples harvested at 24 h. Inhibition of primary infected cells occurred at wortmannin concentrations $>$ 50 nM, with an apparent IC₅₀ of 700 nM (Fig. 1A). No cytotoxicity was observed in the MTT assay at this concentration (data not shown).

Wortmannin treatment also inhibited HIV-1 release from chronically infected U937 cells. Inhibition occurred at concentrations $>$ 50 nM. The IC₅₀ was \approx 300 nM (Fig. 1A), and no cytotoxicity was observed (data not shown). We additionally investigated the effects of another MLCK inhibitor, KT5926 (20, 21), on HIV-1 release in cultures of primary infected H9 cells. KT5926 treatment resulted in a concentration-dependent inhibition of HIV-1 release like that of wortmannin with an apparent IC₅₀ of 1 μ M (Fig. 1A Inset). This IC₅₀ value corresponds to the value for MLCK reported previously (20). These results indicate that inhibition of MLCK suppresses HIV-1 release from both T-cell and monocyte cell lines and is effective in *in vitro* assays using both primary and chronically infected cells.

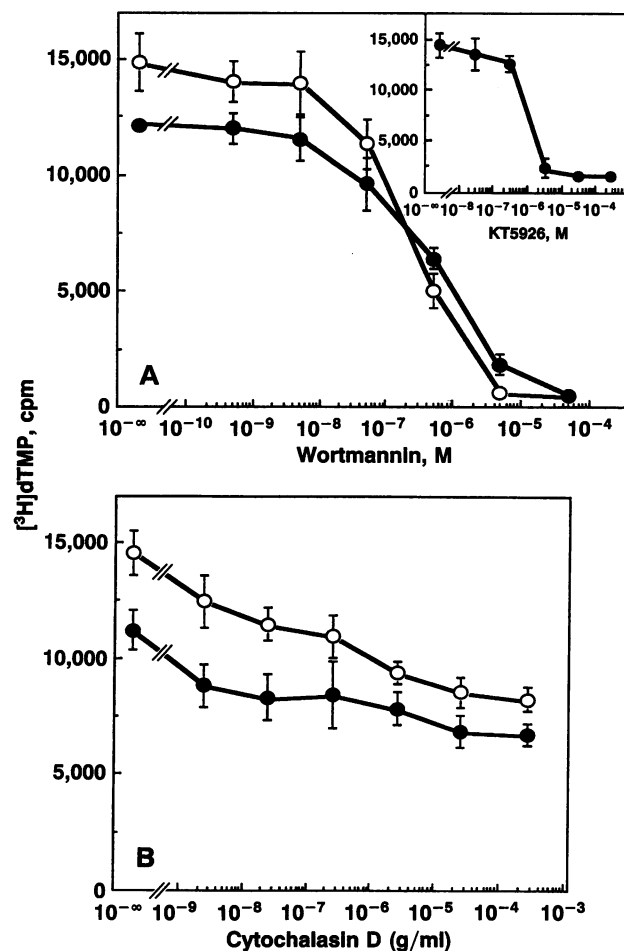


FIG. 1. Inhibitory effects of wortmannin, KT5926, and cytochalasin D on HIV-1 release. Various concentrations of wortmannin (A), KT5926 (A Inset), or cytochalasin D (B) were applied to primary infected H9 cells (●) or chronically infected U937 cells (○). Vertical axis indicates RT activity in the supernatant fraction. Cells were incubated with the agents at 37°C for 24 h prior to measurement of extracellular RT activity.

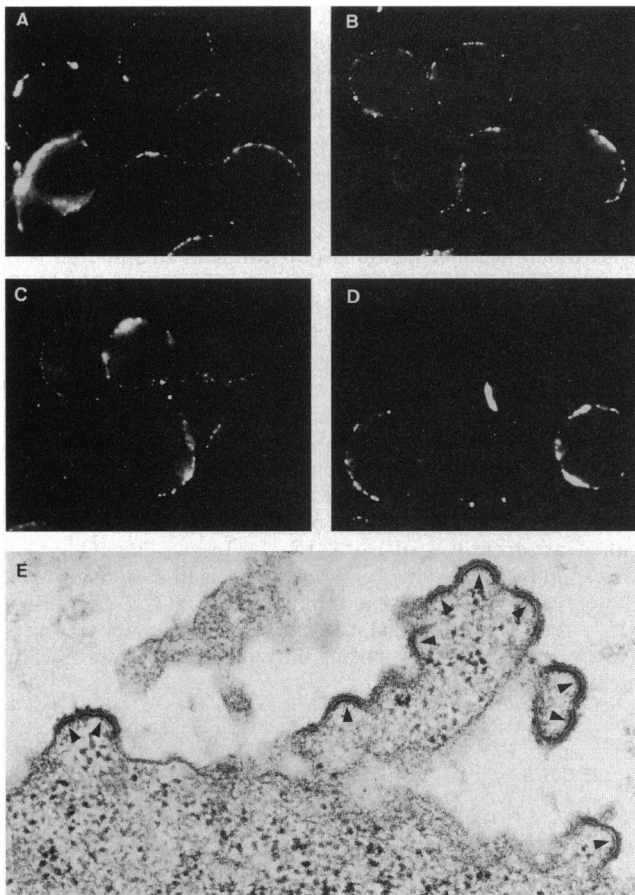


FIG. 2. HIV-1 in H9 cells in the presence or absence of wortmannin. (A–D) Immunofluorescence images. (A and C) Cells treated with 5 μ M wortmannin for 24 h. (B and D) Cells cultured in the absence of wortmannin. (A and B) Primary infected H9 cells at the budding stage were incubated with anti-HIV-1 envelope glycoprotein gp120 antibody and FITC-labeled secondary antibody. (C and D) Cells were incubated with anti-HIV-1 capsid protein p24 antibody and FITC-labeled secondary antibody. Viral proteins were localized in the plasma membrane in the presence (A and C) or absence (B and D) of wortmannin. ($\times 700$.) (E) An electron micrograph of primary infected H9 cells treated with 5 μ M wortmannin for 24 h. Many crescent-shaped HIV-1 nucleoids (arrowheads) stayed underneath the plasma membrane where viral envelope proteins were expressed without stalk formation and budding. ($\times 50,400$.)

Since wortmannin is an effective MLCK inhibitor at concentrations of 300–700 nM, the inhibition of HIV-1 budding at these concentrations suggests that MLCK-mediated phosphorylation of myosin and subsequent myosin–actin interactions might participate in the release of nascent viral particles from the host cells. To explore the role of actin in HIV-1 release, we examined the effects of cytochalasin D on viral release from infected H9 and U937 cells. As shown in Fig. 1B, cytochalasin D inhibited HIV-1 release in a concentration-dependent manner from both H9 and U937 cells, although its inhibition was relatively weak. Cytochalasin D at 25 μ g/ml showed $\approx 38\%$ inhibition of release from H9 cells and 41% from U937 cells with no cytotoxicity. Since cytochalasin D only partially depolymerizes actin filaments, it is impossible to get complete inhibition, but a partial block was obtained.

Since wortmannin was effective in inhibiting HIV-1 production when applied to cells after acute infection and to chronically infected cells, its site of action could be at any step from reverse transcription to budding. To examine further the effect of wortmannin, we used monoclonal antibodies recognizing the HIV-1 envelope glycoprotein gp120 or the HIV-1

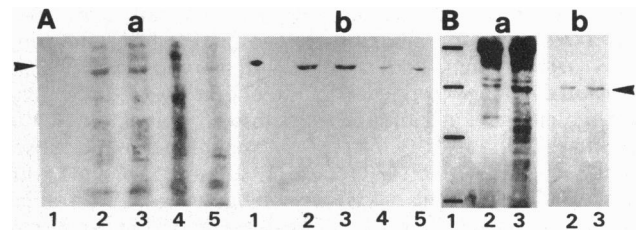


FIG. 3. Immunoblot analysis for confirmation of the presence of myosin and actin in H9 and U937 cells. Lanes: a, protein staining; b, immunostaining. (A) Anti-myosin antibody and a 6% gel. Lanes: 1, chicken gizzard myosin; 2, noninfected H9 cells; 3, infected H9 cells; 4, noninfected U937 cells; 5, infected U937 cells. Arrowhead is at 200 kDa. Gizzard myosin was strongly labeled by immunostaining at a protein concentration too low to detect by protein staining (lane a1). (B) Anti-actin antibody and 14% gel. Lanes 1, molecular mass markers; 2, uninfected H9 cells; 3, uninfected U937 cells. Arrowhead is at 42 kDa. Molecular mass markers are 67 kDa, 42 kDa, 30 kDa, and 20 kDa.

capsid protein p24 to determine the location of these proteins in the primarily infected H9 and chronically infected U937 cells after a 24-h treatment with 5 μ M wortmannin. As shown in Fig. 2 A–D, immunofluorescence microscopy detected these viral proteins on the plasma membrane in the presence or absence of wortmannin. Many fluorescent spots in the infected cells with (Fig. 2A and C) or without (Fig. 2B and D) high concentrations of wortmannin were detected on the plasma membrane in the same way. Viral proteins might remain on the plasma membrane due to an inability to bud in the presence of wortmannin. In the electron microscopic image of primary infected H9 cells exposed to 5 μ M wortmannin (Fig. 2A), many electron-dense crescent-shaped HIV-1 nucleoids stayed underneath the plasma membrane where viral envelope proteins were already expressed, but there was neither stalk formation nor budding (Fig. 2E). The electron microscopic image of an infected H9 cell without wortmannin as a control showed the usual nascent viral particles in the budding state sometimes with stalks but did not exhibit the accumulation of viral components on the plasma membrane as described above (data not shown). These data indicate that the wortmannin did not block the synthesis or transport of viral proteins to the plasma membrane but did inhibit the stalk formation necessary for release of virus particles from the cells.

To obtain further evidence for the participation of myosin and actin in HIV-1 budding, we examined the distribution of myosin and actin in the cells by using a polyclonal antibody that recognizes nonmuscle myosin heavy chain and a monoclonal antibody that recognizes various cytoplasmic actins. We first established the presence of myosin and actin in H9 and U937 cells by immunoblot analysis. As shown in Fig. 3A, the presence of myosin in both cells was confirmed by the specific staining of a single band of 200 kDa. The amount of myosin seemed to be approximately the same in infected and noninfected cells. The presence of actin in noninfected H9 and U937 cells was also confirmed by the appearance of a single band of 42 kDa in immunoblots probed with an anti-actin antibody (Fig. 3B).

Next, we used fluorescence microscopy with the anti-myosin and anti-actin antibodies to determine the distribution of myosin and actin during the budding stage of H9 cells. The distribution of HIV-1 particles was determined in the same cells by the dual-label immunofluorescence method with a polyclonal anti-HIV-1 antibody. As shown in Fig. 4, the dual fluorescence method allowed viral particles to be visualized as dots on the plasma membrane especially as dense spots at the budding region (Fig. 4B and D, arrowheads) and demonstrated that myosin and actin are colocalized at the budding sites of viral particles. In particular, myosin was concentrated

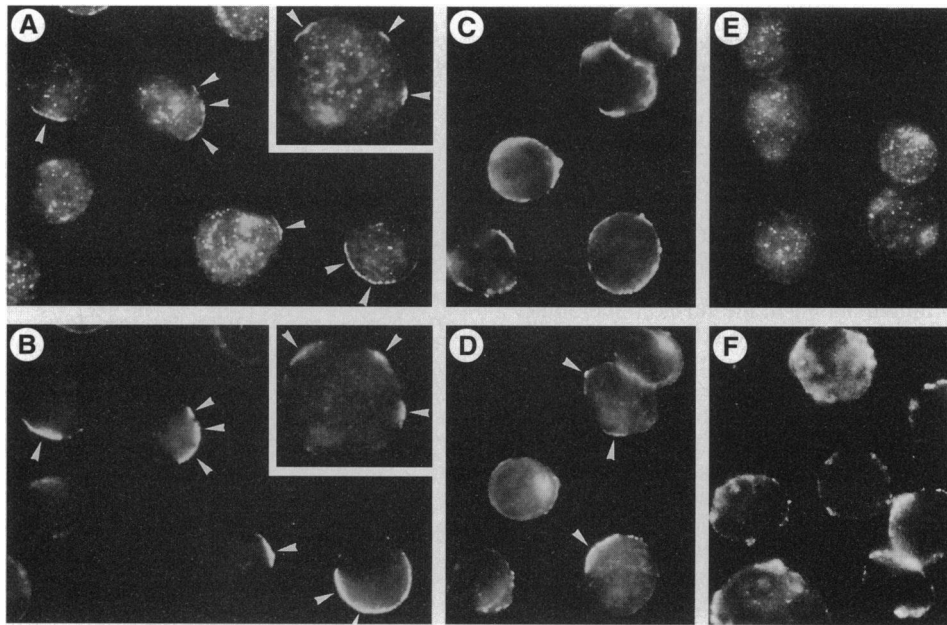


FIG. 4. Colocalization of myosin, actin, and HIV-1 in infected and noninfected H9 cells. (*A* and *B*) Dual-fluorescence image of primary infected H9 cells showing myosin labeled by anti-myosin and a FITC-conjugated secondary anti-rabbit IgG (*A*) and HIV-1 labeled by anti-HIV-1 particle and rhodamine-conjugated secondary anti-mouse IgG (*B*). Myosin was located on the plasma membrane (*A*) (arrowheads) just at sites where HIV-1 particles were budding from the cell surface (*B*) (arrowheads). (*A* and *B* Insets) One cell at higher magnification. (*C* and *D*) Dual-fluorescence image of primary infected H9 cell showing actin labeled by anti-actin and FITC-conjugated secondary anti-rabbit IgG (*C*) and HIV-1 labeled by anti-HIV-1 particle and rhodamine-conjugated secondary anti-mouse IgG (*D*). Actin was distributed throughout the plasma membrane from which HIV-1 particles were budding at the specific sites on the cell surface (arrowheads). (*E* and *F*) Single-fluorescence image of noninfected H9 cells showing myosin or actin labeled by anti-myosin or anti-actin and FITC-conjugated secondary antibody. (*E*) Myosin was randomly distributed in the cytoplasm as small dots and plaques. (*F*) Actin was distributed mainly under the plasma membrane. (*A–F*, $\times 650$; *A* and *B* Insets, $\times 1050$.)

on the same area of the plasma membrane as the dense spots of the viral particles (Fig. 4 *A* and *B*, arrowheads). In contrast, actin was widely distributed on the plasma membrane and was always found in areas where viral particles were present (Fig. 4 *C* and *D*). In the noninfected cells, myosin was visualized randomly in the cytoplasm in the form of small dots and plaques, and actin was localized mainly on the membrane (Fig. 4 *E* and *F*). So that myosin was translocated to the budding region on the surface membrane in the infected cell from the cytoplasm.

To determine the distribution of myosin during the budding stage in greater detail, we used immunoelectron microscopy on HRP-stained cells treated with anti-myosin antibody and HRP-conjugated anti-rabbit IgG. As shown in Fig. 5 *A* and *B*, the presence of myosin was demonstrated as areas of dense stain where viral particles were in the process of budding out from the plasma membrane. In particular, as shown in Fig. 5 *A*, the densely stained stalk-like structure of the membrane on which the budding viral particle was situated indicated the presence of a high concentration of myosin molecules. The density of this region was faint in the control samples stained in the absence of the first antibody (Fig. 5 *C*). Another dense spot in the cytoplasm might indicate location of myosin in the cytoplasm as shown in Fig. 4 *E*.

Release of the nascent virus by budding from the host cell is a very dynamic process, and its molecular mechanism has not yet been elucidated. By using wortmannin, an effective MLCK inhibitor, our group reported the inhibition of acetylcholine release from sympathetic ganglion cell (8) and catecholamine release from chromaffin cells (5, 7). The IC_{50} values for wortmannin in these cases were similar to those determined in this study and the previous work (9), 300 nM to 1 μ M. Our group has also found that wortmannin inhibits phosphatidylinositol 3-kinase at very low concentrations (IC_{50} values of several nanomolar; ref. 25) compared to the inhibition of MLCK. However, we identified the target of wortmannin in the present experiment as MLCK from the IC_{50} for inhibition of HIV-1 production. Additionally another MLCK inhibitor, KT5926, also inhibited the viral release as did wortmannin. Although KT5926 acts on both MLCK and calcium/calmodulin kinase II (21), such an inhibition suggests that it acts mainly on MLCK because of its IC_{50} value in the present work.

By using anti-myosin antibodies that cross-react with non-muscle myosin heavy chain, our group has studied transmitter release from sympathetic ganglionic cells (8) and acid secretion from gastric parietal cells (ref. 6, and Y.N., unpublished work). Localization of myosin on the plasma membrane was observed in both of these studies.

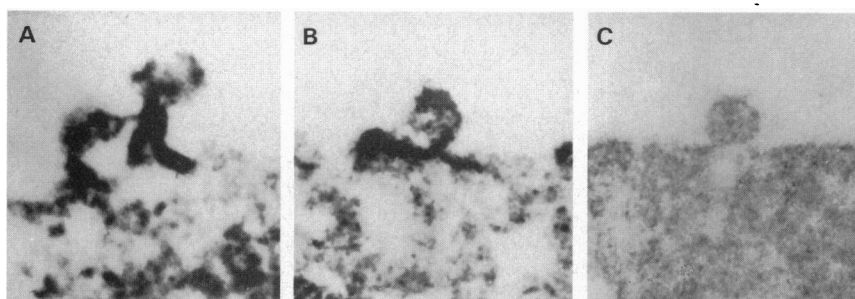


FIG. 5. Localization of myosin in infected H9 and U937 cells by immunoelectron microscopy. The location of myosin is indicated by the HRP reaction products. (*A*) A primary infected H9 cell. (*B*) A chronically infected U937 cell. (*C*) A primary infected H9 cell stained in the absence of the primary antibody as a control ($\times 71,500$.)

In the present study, we have shown that wortmannin inhibited the release of HIV-1 from the host cell but did not inhibit the synthesis or transport of envelope and capsid proteins to the plasma membrane. Thus, wortmannin suppressed only the final process of HIV-1 expression, stalk formation to release infectious viral particles by budding. Consistent with this idea, we were able to demonstrate the presence of myosin just under budding viral particles by using dual-label immunofluorescence microscopy and in stalk-like structures of the plasma membrane by using immunoelectron microscopy.

Actin was also distributed mainly in the surface membrane, and cytochalasin D partially blocked the HIV-1 release. The present result of incomplete inhibition with cytochalasin D suggests that the dynamic polymerization/depolymerization of actin alone is relatively unimportant in HIV-1 budding, but that in the stalk formation or budding, the myosin-actin interaction through stable cytochalasin-resistant actin filaments is much more important. Thus, the actin might participate with myosin in an active process leading to the release of viral particles from the membrane. However, in the transport process of viral components, we cannot rule out the dynamic participation of actin, as has been identified with paramyxoviruses (11–13).

Since the MLCK activation and the initiation of a myosin-actin interaction requires an increase in free intracellular $[Ca^{2+}]_i$ ($[Ca^{2+}]_i$), an increase in $[Ca^{2+}]_i$ that occurs during budding and is accompanied by the phosphorylation of myosin light chain remained to be demonstrated. However, compared to the stimulus-induced exocytosis in neuronal cells, it may be difficult to detect an increase of $[Ca^{2+}]_i$ and the phosphorylation of myosin light chains in the present system, because the budding mechanism is going on continuously and slowly in a very narrow region without any synchronization. In a preliminary experiment, HIV-1 release was suppressed most pronouncedly when both $[Ca^{2+}]_i$ and extracellular calcium ($[Ca^{2+}]_o$) were chelated with bis(2-aminophenoxy)ethane-*N,N,N',N'*-tetraacetic acid (BAPTA) and with EGTA, respectively. The suppression of the release was remarkable when only $[Ca^{2+}]_o$ was chelated with EGTA. The suppression was weak when only $[Ca^{2+}]_i$ was chelated with BAPTA. From these results, we suggest that $[Ca^{2+}]_o$ might enter the cell by the stimulation of viral budding itself at the budding site.

Based upon the results of this study we propose that a myosin-actin interaction plays an important role in HIV budding preceded by the activation of myosin by phosphorylation of the 20-kDa myosin light chain. Furthermore, we believe that these observations suggest an approach to the medical treatment of acquired immunodeficiency syndrome from HIV infection. For example, the chemical modification of wortmannin to reduce its general toxicity may lead to the development of a class of drugs that inhibit the release of HIV from infected cells.

We thank Dr. David Saffen for reading the manuscript and for useful discussions. This work was supported by grants in Aid for Scientific Research from the Ministry of Education, Science and Culture of Japan.

1. Wong-Staal, F. (1989) in *Retroviruses and Disease*, eds. Hanafusa, H., Pinter, A. & Pullman, M. E. (Academic, San Diego), pp. 148–158.
2. Geelen, J. L. M. C. & Goudsmit, J. (1991) in *Progress in Medical Virology*, ed. Melnick, J. L. (Karger, Basel), pp. 27–41.
3. Vaishnav, Y. N. & Wong-Staal, F. (1991) *Annu. Rev. Biochem.* **60**, 577–630.
4. Kitani, S., Teshima, R., Morita, Y., Ito, K., Matsuda, Y. & Nonomura, Y. (1992) *Biochem. Biophys. Res. Commun.* **183**, 48–54.
5. Ohara-Imaizumi, M., Sakurai, T., Nakamura, S., Nakanishi, S., Matsuda, Y., Muramatsu, S., Nonomura, Y. & Kumakura, K. (1992) *Biochem. Biophys. Res. Commun.* **185**, 1016–1021.
6. Nonomura, Y. (1993) *Biomed. Res.* **14**, Suppl. 2, 107–112.
7. Kumakura, K., Sasaki, K., Sakurai, T., Ohara-Imaizumi, M., Misonou, H., Nakamura, S., Matsuda, Y. & Nonomura, Y. (1994) *J. Neurosci.* **14**, 7695–7703.
8. Mochida, S., Kobayashi, H., Matsuda, Y., Yuda, Y., Muramoto, K. & Nonomura, Y. (1994) *Neuron* **13**, 1131–1142.
9. Nakanishi, S., Kakita, S., Takahashi, I., Kawahara, K., Tsukuda, E., Sana, T., Yamada, K., Yoshida, M., Kase, H., Matsuda, Y., Hashimoto, Y. & Nonomura, Y. (1992) *J. Biol. Chem.* **267**, 2157–2163.
10. Korn, E. D. (1982) *Physiol. Rev.* **62**, 672–737.
11. Stallcup, K. C., Raine, C. S. & Fields, B. N. (1983) *Virology* **124**, 59–74.
12. Bohn, W., Rutter, G., Hohenberg, H., Mannweiler, K. & Nobis, P. (1986) *Virology* **149**, 91–106.
13. Mayer, S. A., Baker, S. C. & Horikami, S. M. (1990) *J. Gen. Virol.* **71**, 775–783.
14. Brenner, S. L. & Korn, E. D. (1979) *J. Biol. Chem.* **254**, 9982–9985.
15. Brown, S. S. & Spudich, J. A. (1979) *J. Cell Biol.* **83**, 657–662.
16. Flanagan, M. D. & Lin, S. (1980) *J. Biol. Chem.* **255**, 835–838.
17. Lin, D. C., Tobin, K. D., Grumet, M. & Lin, S. (1980) *J. Cell Biol.* **84**, 455–460.
18. Cooper, J. A. (1987) *J. Cell Biol.* **105**, 1473–1478.
19. Gottlieb, T. A., Ivanov, I. E., Adesnik, M. & Sabatini, D. D. (1993) *J. Cell Biol.* **120**, 695–710.
20. Nakanishi, S., Yamada, K., Iwahashi, K., Kuroda, K. & Kase, H. (1990) *Mol. Pharmacol.* **37**, 482–488.
21. Hashimoto, Y., Nakayama, T., Teramoto, T., Kato, H., Watanabe, T., Kinoshita, M., Tsukamoto, K., Tokunaga, K., Kurokawa, K., Nakanishi, S., Matsuda, Y. & Nonomura, Y. (1991) *Biochem. Biophys. Res. Commun.* **181**, 423–429.
22. Hoffman, A. D., Banapour, B. & Levy, J. A. (1985) *Virology* **147**, 326–335.
23. Twentyman, P. R. & Luscombe, M. (1987) *Br. J. Cancer* **56**, 279–285.
24. Ohno, T., Terada, M., Yoneda, Y., Shea, K. W., Chambers, R. F., Stroka, D. M., Nakamura, M. & Kufe, D. W. (1991) *Proc. Natl. Acad. Sci. USA* **88**, 10726–10729.
25. Yano, H., Nakanishi, S., Kimura, K., Hanai, N., Saitoh, Y., Fukui, Y., Nonomura, Y. & Matsuda, Y. (1993) *J. Biol. Chem.* **268**, 25841–25850.